

## D. STRUCTURE OF NUCLEI FAR FROM STABILITY

A core issue in nuclear structure research concerns the evolution of nuclear behavior as one moves away from stability by varying the neutron-to-proton ratio. Traditional shell gaps are shown to disappear and new gaps arise. The exact origins of these phenomena still have to be fully understood, though modification of the spin-orbit effect and other residual interactions appears likely. We continue to probe nuclei along the proton dripline from light masses to heavy. In addition, our efforts to reach neutron-rich nuclei have grown, through fragmentation experiments, traditional fusion of very neutron-rich species, and using multi-nucleon transfer.

### d.1. Neutron-Rich Nuclei

#### d.1.1. High Spin Structure in Neutron-Rich Ti and Cr Isotopes: Possible N = 32 and 34

**Shell Gaps and the Onset of Deformation** (R. V. F. Janssens, S. Zhu, M. P. Carpenter, F. G. Kondev, C. J. Lister, N. J. Hammond, T. Lauritsen, D. Seweryniak, P. Chowdhury, ‡ D.-C. Dinca,\* A. Gade,\* D. Bazin,\* C. M. Campbell,\* J. M. Cook,\* T. Glasmacher,\* J.-L. Lecouey,\* S. N. Liddick,\* P. F. Mantica,\* W. F. Mueller,\* H. Olliver,\* J. R. Terry,\* B. A. Tomlin,\* K. Yoneda,\* S. J. Freeman, § A. Deacon, § J. F. Smith, § B. J. Varley, § R. Broda, † and B. Fornal †)

Over the last few years, our collaboration has initiated a program to investigate the properties of neutron-rich nuclei above doubly-magic  $^{48}\text{Ca}$ . At the onset, the primary motivation for these studies was the expectation that substantial modifications can occur to the intrinsic shell structure of nuclei with a sizable neutron excess.<sup>1</sup> Alterations to the energy spacings of the orbitals and/or to their ordering can have a considerable impact on global nuclear properties such as the nuclear shape or the type of excitations characterizing the low-energy level spectra.

Our approach has been one where we combine beta decay and intermediate-energy Coulomb excitation measurements performed at the NSCL with deep inelastic reactions or fusion-evaporation with radioactive targets carried out with Gammasphere at ATLAS. Our main results can be summarized as follows:

(1) Following first indications of the onset of a N = 32 sub-shell gap in  $^{56}\text{Cr}$ ,<sup>2</sup> we have demonstrated the power of combining techniques and accelerators by firmly establishing the N = 32 sub-shell in  $^{54}\text{Ti}$ .<sup>3</sup> This gap manifests itself through the high energy of the first excited  $2^+$  state and the large energy gap between the lowest  $6^+$  level and higher spin states (which reflects the high energy cost of promoting

neutrons across the gap). The data were found to be in good agreement with shell model calculations using the recently developed GXPF1 effective interaction which accounts for the N = 32 gap by the combined action of a weakening of the  $\pi[1f_{7/2}] - \nu[1f_{5/2}]$  proton-neutron monopole interaction as protons are removed from the  $1f_{7/2}$  orbital (filled at Z = 28) and a significant  $\nu(2p_{1/2} - 2p_{3/2})$  spin-orbit splitting.

(2) With the same combined techniques, we subsequently studied  $^{56}\text{Ti}$  and discovered (a) from beta decay that its first excited  $2^+$  state is much lower in excitation energy than the corresponding state in  $^{54}\text{Ti}$ ,<sup>4,5</sup> and (b) from deep inelastic reactions<sup>6</sup> that the higher excitations do not show any indication of a shell gap at N = 34, contrary to predictions based on shell model calculations with the GXPF1 interaction.

(3) To place the interpretation above on firmer ground, the B(E2;  $0^+ \rightarrow 2^+$ ) reduced transition probabilities were measured for the  $^{52-56}\text{Ti}$  even isotopes.<sup>7</sup> From Fig. I-20, a clear anti-correlation between two observables can be readily seen: while the  $2^+$  energies increase significantly at N = 28 and N = 32 the B(E2) strengths are lowest for these two neutron numbers. Furthermore, both these physical quantities also differ markedly from the corresponding values at neutron numbers N = 26, 30 and 34. For  $^{50}\text{Ti}$ , the well known shell closure at N = 28 translates into a

small transition probability: with the  $B(E2)$  value of Fig. I-20(b), the deexcitation from the  $2^+$  level to the ground state has a strength of only 5.6 single-particle units. The fact that the excitation energy and the reduced transition probability observed in  $^{54}\text{Ti}$  are comparable to those in  $^{50}\text{Ti}$  then confirms that the Ti isotope with  $N = 32$  is as good a semi-magic nucleus as its  $N = 28$  counterpart and, hence, that a substantial sub-shell gap must occur at  $N = 32$ . Conversely, the fact that the three other Ti isotopes have  $2^+$  excitation energies lower by several hundreds of

keV and  $B(E2)$  values higher by a factor of  $\sim 2$  can be interpreted as an experimental indication for the absence of sub-shell gaps in the neutron single-particle spectrum at  $N = 26, 30$  and  $34$ .

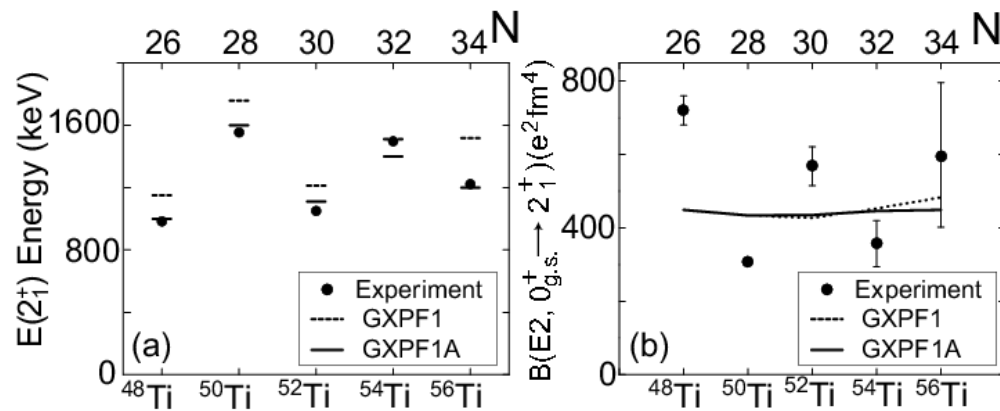


Fig. I-20.  $2^+$  excitation energies and  $B(E2)$  transition probabilities compared to shell model calculations with the GXPF1 and the GXPF1A interactions.

The results summarized above have led to further theoretical work, both in the framework of the shell model and with other approaches. Specifically, our results have led to a modified version of the interaction, labeled GXPF1A, in which the matrix elements of the interaction involving mostly the  $p_{1/2}$  orbital have been readjusted. It is worth pointing out that the evaluation of the properties of this orbital from experimental data is particularly challenging since it contributes little angular momentum to any given state. Traces of its impact are often obscured as a result. The solid lines in Fig. I-20(a) indicate that the GXPF1A calculations reproduce the  $E(2^+)$  energies. In fact, they provide a satisfactory description of all the known levels in the even Ti nuclei, including those above the  $6^+$  level in  $^{54}\text{Ti}$  which involve neutron excitations across the  $N = 32$  shell. They also describe the odd Ti nuclei satisfactorily.<sup>8</sup> We note that the calculations do not reproduce the  $B(E2)$  probabilities very well. This may well be due to the poor knowledge we have at present of the values of the effective charges to be used.

The success of the GXPF1A interaction depends also sensitively on the size of the neutron gap at  $N = 40$ . A large  $N = 40$  gap effectively isolates the low-lying structure from the neutron  $g_{9/2}$  state, whereas a weak shell closure facilitates excitations involving this shape-driving orbital. The Cr isotopes lie in the middle of the  $\pi f_{7/2}$  shell and could potentially display some of the strongest collective effects.

Our collaboration has been investigating the Cr nuclei of interest as well, and so far, we have carried out a number of investigations of the neutron-rich Cr nuclei. At the NSCL, beta decay into some of the nuclei of interest has been studied.<sup>1</sup> Based on the latter, yrast and near-yrast level structures in  $^{56}\text{Cr}$  and  $^{58}\text{Cr}$  have been delineated from deep inelastic data measured with Gammasphere following the  $^{48}\text{Ca} + ^{208}\text{Pb}$  and  $^{48}\text{Ca} + ^{238}\text{U}$  reactions.<sup>9</sup> To obtain the level structure of  $^{60}\text{Cr}$  as well as that of the odd  $^{57,59}\text{Cr}$  isotopes, another approach was used at ATLAS with Gammasphere and the Fragment Mass Analyzer (FMA). The  $^{14}\text{C}(^{48}\text{Ca}, 2p)^{60}\text{Cr}$  fusion-evaporation reaction with a  $^{14}\text{C}$  radioactive target has a very small cross section (neutron-rich compound nuclei are 100-1000 times more likely to evaporate neutrons), but with the

selectivity of the FMA it was possible to identify the relevant transitions with Gammasphere.<sup>9</sup> From the same experiment, the level scheme of <sup>57</sup>Cr was obtained as well.<sup>10</sup> The same experimental approach, but with the <sup>13</sup>C(<sup>48</sup>Ca,2p)<sup>59</sup>Cr reaction, has provided the recently published <sup>59</sup>Cr level structure.<sup>11</sup>

The <sup>57,59,60</sup>Cr level schemes are given in Fig. I-21, while the 2<sup>+</sup> excitation energies for the N = 26-38 Cr isotopes are summarized in Fig. I-22. As can be seen from Fig. I-22, the N = 32 shell gap discussed above for the Ti isotopes is present in the Cr nuclei as well, but the effect is less pronounced, as one would expect since two additional protons occupy the f<sub>7/2</sub> shell and the π[1f<sub>7/2</sub>] - ν[1f<sub>5/2</sub>] proton-neutron monopole interaction is correspondingly stronger. In fact, the latest GXPF1A interaction accounts for the level structure of the N = 28-34 nuclei quite well<sup>9</sup> (not shown). However, from Fig. I-21, it is evident that the situation changes drastically for N = 35, 36. Remarkably, the 2<sup>+</sup> energy drops considerably at N = 36: to 645 keV from 1007 and 880 keV in <sup>56</sup>Cr and <sup>58</sup>Cr, respectively. In addition, the <sup>60</sup>Cr level structure of Fig. I-21 differs quite markedly from that of the lighter even isotopes (not shown): the transition energies involved are lower and, while the 6<sup>+</sup>→4<sup>+</sup>→2<sup>+</sup>→0<sup>+</sup> cascade can hardly be characterized as rotational, it nevertheless shows a degree of regularity not seen in the lighter even Cr isotopes with the transition energies increasing with spin. In addition, the <sup>60</sup>Cr level structure cannot be reproduced by shell model calculations with the GXPF1A interaction. These observations parallel those made when we studied <sup>59</sup>Cr (Fig. I-21). Here

too, the level structure could not be accounted for with the GXPF1A interaction.<sup>11</sup> It is quite possible that deformation needs to be considered in the interpretation of <sup>59</sup>Cr and <sup>60</sup>Cr. A striking feature of <sup>59</sup>Cr level structure is the presence of the long-lived 9/2<sup>+</sup> level at low excitation energy. This level is associated with the g<sub>9/2</sub> neutron orbital<sup>10,11</sup> which is shape driving. It is shown<sup>11</sup> that, for oblate deformations β<sub>2</sub> < 0.25, the g<sub>9/2</sub> orbital falls dramatically in energy towards the Fermi surface and one can achieve a qualitative understanding of the <sup>59</sup>Cr level structure. Effects associated with deformation are perhaps even more dramatic in <sup>57</sup>Cr,<sup>10</sup> where a rotational cascade can be observed on top of a 9/2<sup>+</sup> level. It is shown<sup>10</sup> that this sequence can be understood in the framework of TRS calculations as a rotational band with prolate deformation induced by the excitation of the odd (N = 33) neutron into the 1/2<sup>+</sup>[440] of g<sub>9/2</sub> parentage. The calculations reproduced all the observed features, including a strong gain in alignment at high spin. The calculations also account for a similar, but less well developed structure in <sup>55</sup>Cr.<sup>10</sup>

The picture that emerges thus far for the odd Cr isotopes is that the excitation of a g<sub>9/2</sub> neutron is sufficient to polarize the soft core into a deformed shape. In <sup>55,57</sup>Cr, the low-lying negative-parity states appear to be roughly spherical in nature and the νg<sub>9/2</sub> excitation produces a prolate shape and a decoupled band. In <sup>59</sup>Cr, a prolate shape is incompatible with the isomeric nature of the 9/2<sup>+</sup> state and it appears that the excitation of a g<sub>9/2</sub> neutron drives an already mildly oblate core towards oblate deformation. The latter deformation then also characterizes <sup>60</sup>Cr.

\*Michigan State University, †Niewodniczanski Institute of Nuclear Physics, Krakow, Poland, ‡University of Massachusetts-Lowell, §University of Manchester, United Kingdom.

<sup>1</sup>B. A. Brown, Prog. in Part. and Nucl. Phys. **47**, 517 (2001).

<sup>2</sup>J. I. Prisciandaro *et al.*, Phys. Lett. **B510**, 17 (2001).

<sup>3</sup>R. V. F. Janssens *et al.*, Phys. Lett. **B546**, 55 (2002).

<sup>4</sup>S. N. Liddick *et al.*, Phys. Rev. Lett. **92**, 072502 (2004).

<sup>5</sup>S. N. Liddick *et al.*, Phys. Rev. C **70**, 064303 (2004).

<sup>6</sup>B. Fornal *et al.*, Phys. Rev. C **70**, 064304 (2004).

<sup>7</sup>D.-C. Dinca *et al.*, Phys. Rev. C **71**, 041302(R) (2005).

<sup>8</sup>B. Fornal *et al.*, Proceedings 8th Spring Seminar on Nuclear Physics, Paestum, Italy, May 2004, to be published.

<sup>9</sup>S. Zhu *et al.*, to be published.

<sup>10</sup>A. N. Deacon *et al.*, submitted to Phys. Lett. B.

<sup>11</sup>S. J. Freeman *et al.*, Phys. Rev. C **69**, 064301 (2004).

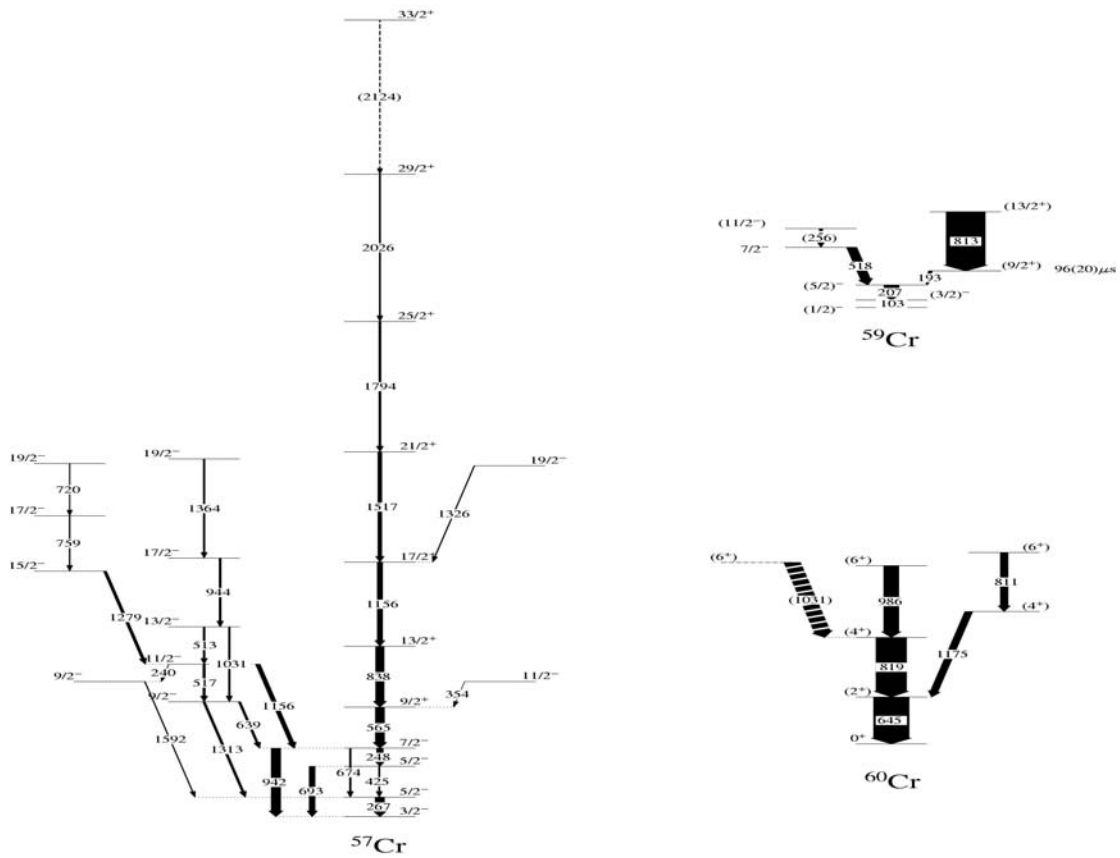


Fig. I-21. Preliminary level schemes for  $^{57,59,60}\text{Cr}$  obtained with Gammasphere and the FMA.

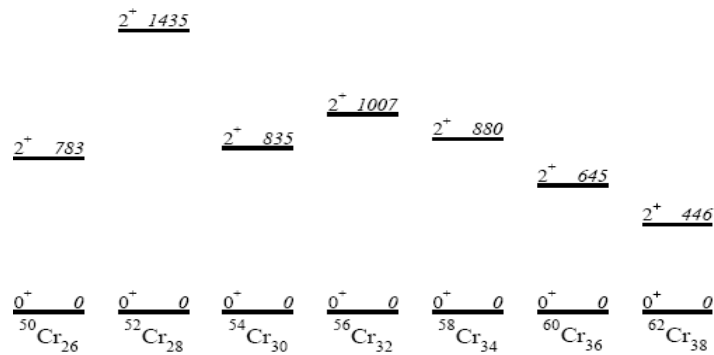


Fig. I-22. Systematics of the  $2^+$  energies for the Cr isotopes.

### d.1.2. Search for $^{82}\text{Ge}_{50}$ Using Deep Inelastic Reactions (M. P. Carpenter, F. G. Kondev, R. V. F. Janssens, T. L. Khoo, T. Lauritsen, C. J. Lister, D. Seweryniak, and S. Zhu)

The study of doubly and semi magic nuclei have historically proven to be important in establishing for example the parameter strengths for the shell model. Until recently, these parameters were set by nuclei lying near the line of beta-stability, however, with the coming online of a number of first and second generation radioactive beam facilities, studies of exotic neutron rich nuclei at and near closed shells have begun. What has motivated many of these measurements from a nuclear structure standpoint is the fact that rearrangements of single-particle energies are observed for neutron rich. Such changes in the single-particle energies have been attributed to the attractive strength of the spin-isospin part of the effective nuclear interaction. As a result, one has observed the disappearance of certain magic numbers and the emergence of new closed shells.

Our collaboration has been actively studying neutron rich nuclei in the Ca-Ti region in order to examine a similar phenomenon. Specifically, we have been investigating Ti and Cr isotopes with  $N > 28$ . Recent shell model calculations using the GXPF1 Hamiltonian had suggested a new closed shell for  $N = 32$  and  $Z \leq 24$  and the emergence of a shell gap at  $N = 34$  for  $Z \leq 22$ .<sup>1</sup> Our recent results from Gammasphere using both the  $^{48}\text{Ca} + ^{208}\text{Pb}$  and  $^{48}\text{Ca} + ^{238}\text{U}$  reactions has confirmed the  $N = 32$  gap for  $^{54}\text{Ti}$  ( $Z = 22$ )<sup>2</sup> and shown that no such gap has developed at  $N = 34$  for  $Z = 22$  ( $^{56}\text{Ti}$ ).<sup>3</sup> Indeed, shell model calculations using the GXPF1 Hamiltonian do an excellent job in reproducing the excitation energy of levels up to  $I = 10 \hbar$  in  $^{50,52,54}\text{Ti}$  but fail for the  $^{56}\text{Ti}$  case. We also note that the study of the high-spin properties of  $^{54,56}\text{Ti}$  were made possible by the previous identification of the  $2^+ - 0^+$  transition in both these nuclei from  $\beta$ -decay of  $^{54,56}\text{Sc}$  produced at the MSU fragmentation facility.<sup>2,4</sup> In addition, we have recently performed Coulomb excitation experiment

on  $^{52,54,56}\text{Ti}$  at MSU in order to measure the  $B(E2)$  rates for the  $2^+ - 0^+$  transition in each isotope and further quantify the magicity of  $^{54}\text{Ti}$ .<sup>5</sup>

With the success of the Gammasphere experiments utilizing a  $^{48}\text{Ca}$  beam to explore the yrast sequences in the neutron rich Ti isotopes, we have extended our measurements into the region around  $N = 50$  and  $Z = 28$  ( $^{78}\text{Ni}$ ). Neutron rich nuclides in this region are of particular interest due to their role in the r-process, and in particular, their contribution to the peak in the solar elemental abundance near  $A = 80$ . While much is known with regards to the  $N = 50$  isotones starting at  $^{86}\text{Kr}$  and proceeding up towards  $^{100}\text{Sn}$ , very little is known about the isotones approaching and including  $^{78}\text{Ni}$ . In the Gammasphere measurement, data were collected using an  $^{82}\text{Se}$  beam incident on both thick  $^{208}\text{Pb}$  and  $^{238}\text{U}$  targets. As a result, all products produced in these reactions are stopped in the target. Data were taken at two different beam energies 525 and 630 MeV. In addition, the time between beam pulses was 400 ns allowing for the identification of isomers with lifetimes as long as several  $\mu$  sec.

One of the main goals of this measurement was to identify the yrast structures for both  $^{84}\text{Se}_{50}$  and  $^{82}\text{Ge}_{50}$  to spins up to  $\sim 12 \hbar$ . In addition, we hoped to develop detailed level structures for  $^{81}\text{Se}$ ,  $^{83}\text{Se}$ ,  $^{83}\text{As}$ ,  $^{81}\text{Ge}$ , and possibly  $^{83}\text{Ge}$ . Two separate "blue" data bases have been created from the data taken at 630 MeV which correspond to the  $^{208}\text{Pb}$  and  $^{238}\text{U}$  targets respectively. Several coincidence cubes have been constructed from these data bases, corresponding to prompt-prompt-prompt, prompt-prompt-delayed and prompt-delayed-delayed transitions. While the analysis is ongoing, current results include a more extensive level scheme for  $^{84}\text{Se}$  than previously known as well as new level schemes for  $^{81}\text{Se}$  and  $^{83}\text{Se}$ . The data is currently under analysis.

<sup>1</sup>J. I. Prisciandaro *et al.*, Phys. Lett. **B510**, 17 (2001).

<sup>2</sup>R. V. F. Janssens *et al.*, Phys. Lett. **B546**, 55 (2002).

<sup>3</sup>B. Fornal *et al.*, Phys. Rev. C **70**, 064304 (2004).

<sup>4</sup>S. Liddek *et al.*, Phys. Rev. Lett. **92**, 072502 (2004).

<sup>5</sup>D.-C. Dinca *et al.*, Phys. Rev. C **71**, 041302 (2005).

**d.1.3. The  $\nu 9/2[404]$  Orbital and the Deformation in the  $A \sim 100$  Region** (I. Ahmad, W. Urban,\* J. A. Pinston,† J. Genevey,† T. Rzaca-Urban,\* A. Zlomaniec,\* G. Simpson,‡ J. L. Durell,§ W. R. Phillips,§ A. G. Smith,§ B. J. Varley,§ and N. Schulz¶)

Levels in  $^{101}\text{Zr}$  were investigated by prompt  $\gamma$ -ray spectroscopy of fission fragments produced in the spontaneous fission of  $^{248}\text{Cm}$ . The measurements were carried out with the EURO GAM2 array of Compton-suppressed Ge detectors. An isomeric level was identified at 941.8 keV in  $^{101}\text{Zr}$  and its half-life was measured to be  $16 \pm 2$  ns. The level is interpreted as a K-isomer corresponding to the  $9/2[404]$  neutron-hole excitation. The level scheme of  $^{101}\text{Zr}$  is shown in Fig. I-23. Several transitions were identified in the  $9/2^+[404]$  rotational band.

Using the cross-over to cascade  $\gamma$ -ray intensities we deduced the  $g_K-g_R/Q_0$  values. Substituting the theoretical value of  $g_K$  and  $g_R = 0.2$  in the expression, we deduced the quadrupole moment  $Q_0 = 3.6(4)$  eb. This quadrupole moment corresponds to a deformation  $\beta_2 = 0.38(4)$ . Similar deformations are observed in  $^{97}\text{Sr}$  and  $^{99}\text{Zr}$ . These deformations and shape changes as a function of neutron number are understood in terms of the single-particle states available in this mass region. The results of this study were published.<sup>1</sup>

\*Warsaw University, Poland, †Institut des Sciences Nucleaires/Universite Josef Fourier, Grenoble, France, ‡Institut Laue-Langevin, Grenoble, France, §University of Manchester, United Kingdom, ¶Institut de Recherches Subatomiques, Strasbourg, France.

<sup>1</sup>W. Urban *et al.*, Eur. Phys. J. A **22**, 157 (2004).

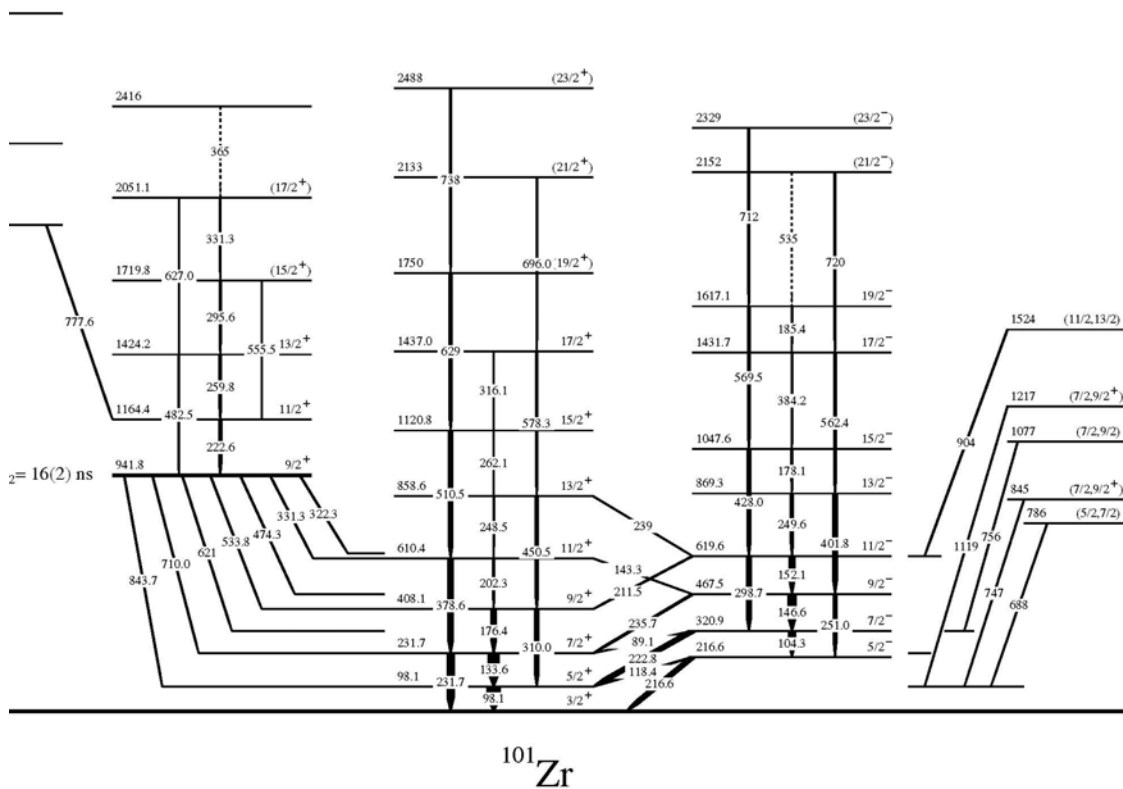


Fig. I-23. A partial level scheme of  $^{101}\text{Zr}$ .

## d.2. Proton-Rich Nuclei

### d.2.1. The $A = 31$ Mirror Nuclei $^{31}\text{P}$ and $^{31}\text{S}$ Used to Investigate the Charge-Symmetry-Breaking “Electromagnetic Spin Orbit” Interaction $V_{\text{eso}}$ (C. J. Lister,

M. P. Carpenter, N. J. Hammond, R. V. F. Janssens, T. L. Khoo, T. Lauritsen, D. Seweryniak, D. G. Jenkins,\* P. Chowdhury,† T. Davinson,‡ P. Woods,‡ A. Jokinen,§ and H. Penttila§)

If nuclear forces were charge symmetric and neutrons and protons had equal mass, charge and magnetic moments, then the spectrum of states mirror pairs of nuclei should be identical. In fact, the spectra are indeed similar, and deviations between mirror partners provide a sensitive probe of our knowledge of nuclear structure. If the position of each level relative to its groundstate is compared, then much of the monopole shift, arising from proton and neutron mass difference and the Coulomb displacement, is removed and subtle differences in structure emerge. These differences are called Mirror Energy Differences (MEDs), the difference  $\Delta E = \{E(J, T_z = -1/2) - E(J, T_z = +1/2)\}$ . In general these MEDs are small, on the order of  $\sim 50$  keV. However, attention has been drawn to some much larger differences. Ekman *et al.* have recently examined the  $T = 1/2$   $A=35$  mirror pair  $^{35}\text{Ar}$  and  $^{35}\text{Cl}^1$  and also reviewed  $T = 1/2$  data from  $A = 33$  to  $A = 39$ . Many interesting effects could be investigated, especially arising in very pure, single-amplitude, shell model configurations. Here, MEDs of several hundred keV were found. The interpretation of these relative shifts was through modern large basis shell model calculations which provide an excellent description of the wavefunctions and allow detailed investigation of charge-symmetry-breaking in the interactions. A key observation was that of the “electromagnetic” spin-orbit effect on the uncoupled last nucleon; the effect of the interaction between its magnetic moment and the magnetic field

induced by motion in the Coulomb field of the nucleus. This effect is completely analogous to the spin-orbit interaction felt by atomic electrons. If this interaction conforms to predictions it should be a rather ubiquitous feature in mirror pairs of nuclei. We have made new measurements on  $^{31}\text{S}$  which allow the  $A = 31$  mirror pair  $^{31}\text{S}$  and  $^{31}\text{P}$  to be added to this investigation, and reveal effects consistent with those reported in Ref. 1.

$^{31}\text{S}$  was produced in the  $^{12}\text{C}(^{20}\text{Ne},n)^{31}\text{S}$  reaction at 32 MeV. The FMA was used to identify the reaction channel, and Gammasphere was used to measure the decays from states in  $^{31}\text{S}$ . Many new levels were found and their spectroscopic properties could be determined. We found the yrast states of  $^{31}\text{S}$  and  $^{31}\text{P}$  showed very small MEDs ( $< 50$  keV), but, as for  $A = 35$ , some stretched configurations showed shifts of the order of  $\sim 250$  keV, consistent with simple expectations of the Electromagnetic Spin orbit Splitting. Our results have been written up in a Rapid Communication to PRC.<sup>2</sup> We are in the process of examining the overall systematics of this effect in known data, and have written a proposal to seek the effect in heavier nuclei, where the orbital angular momentum is bigger, so the effect more clear. However, we have also become more aware of binding energy effects on the Coulomb energy.<sup>3</sup> Quantification of the electromagnetic spin-orbit shifts can only be made after correction for the difference in binding energy of equivalent states in any mirror pair.

\*University of York, United Kingdom, †University of Massachusetts-Lowell, ‡University of Edinburgh, United Kingdom, §University of Jyväskylä, Finland.

<sup>1</sup>J. Ekman *et al.*, Phys. Rev. Lett. **92**, 132502 (2004).

<sup>2</sup>D. G. Jenkins *et al.*, submitted to Phys. Rev C (2005).

<sup>3</sup>J. D. Millener, private communication (2005).

### d.2.2. High Spin States of $T = 3/2$ $^{37}\text{Ca}$ and $^{37}\text{Cl}$ (M. P. Carpenter, C. J. Lister, C. N. Davids, S. Williams,\* P. H. Regan,\* M. A. Bentley,† A. M. Bruce,‡ C. Chandler,† J. Ekman,§ W. Gelletley,† G. Hammond,† D. T. Joss,† D. Rudolph,§ and D. D. Warner¶)

Following the successful investigation of production of  $^{49}\text{Fe}$  (see section d.2.3.) a similar “proof-of-principle” experiment was conducted to investigate the possibility of performing gamma-ray spectro-

scopy on  $T = -3/2$   $^{37}\text{Ca}$  and testing the Isobaric Mass Multiplet Equation in the sd-shell, where traditional shell modeling is at its most sophisticated. The reaction  $^{12}\text{C}(^{28}\text{Si},3n)^{37}\text{Ca}$  was used. Again, absolutely excellent

Z-resolution was achieved, and there is no doubt that sufficient channel selection can be achieved to isolate  $^{37}\text{Ca}$ . The FMA could be set to eliminate almost all

scattered beam. Fig. I-24 shows the Z-separation, just from the ion chamber (1a), and with  $\text{ET}^2$  selection of  $A = 37$  events (1b).

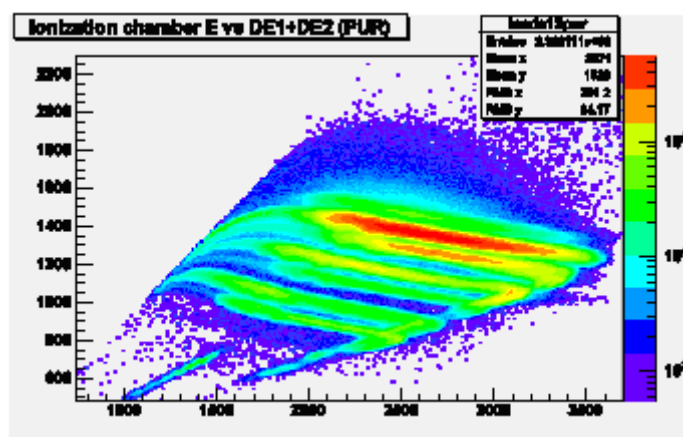


Fig. I-24. Ion Chamber Bragg curves for  $A = 37$  ions stopping in isobutane. The excellent Z-resolution is clear, and loci for  $A = 37$  Ca, K, Ar, and Cl could be identified.

\*University of Surrey, United Kingdom, †Keele University, Staffordshire, United Kingdom, ‡University of Brighton, United Kingdom, §Lund University, Sweden, ¶CLRC Daresbury Laboratory, Warrington, United Kingdom.

### d.2.3. High Spin States in the $N = Z - 3$ Nucleus $^{49}\text{Fe}$ : Coulomb Effects at Large Proton Excess (C. J. Lister, M. P. Carpenter, D. Seweryniak, C. Davids, M. A. Bentley,\* G. Hammond,\* D. D. Warner,† J. Simpson,† R. C. Lemmon,† D. Rudolph,‡ J. Ekman,‡ C. Fahlander,‡ L-L. Andersson,‡ E. Johansson,‡ A. M. Bruce,§ D. Judson,§ M. J. Taylor,§ W. Gelletly,¶ and S. J. Williams¶)

Measuring isobaric mass multiplets and comparing their excited states has had a long history in investigating charge-symmetry breaking effects in nuclear forces. As one moves to heavier nuclei this research continues to raise new issues, especially as the proton dripline is approached. The development of large basis shell models has provided a powerful theoretical tool for this kind of investigation.

$^{49}\text{Fe}$  is a  $T = -3/2$  nucleus about which little is known. Comparing its excited states with more bound isobars will provide a spin-dependent test of the Isobaric Mass Multiplet Equation. However, it is a cutting-edge challenge to obtain data on this nucleus. A test experiment was performed to investigate if spectroscopy is feasible.

The key issues were (a) Can  $^{49}\text{Fe}$  be produced at a rate which allows spectroscopy with Gammasphere? (b) Can sufficiently clean isotope identification be

achieved to produce clean gamma-ray spectra of nuclei produced at the  $1/4$  mb level? (c) Can these conditions be achieved given the use of degrader foils, located downstream of the target, which were required due to the very high recoil velocity?

The experiment was performed as an FMA stand-alone experiment, but with one clover gamma-ray detector located at 90 to the beam direction. The FMA focal plane detectors consisted of a micro-channel plate detectors for determination of position ( $A = Q$ ) and a ionization chamber, for Z-identification through measurement of energy loss and total energy of the recoils. A 230 MeV  $^{40}\text{Ca}$  beam impinged on a  $0.26 \text{ mg/cm}^2$   $^{12}\text{C}$  target. The recoils, which had an energy of around 160 MeV, were slowed down in degrader foils located between 9 and 12 cm downstream of the target. This was necessary in order to reduce the recoil energy into a range that would be deflected by an electric field corresponding to the maximum achievable voltage on the FMA electric



dipoles. The FMA focal plane slits were wound in to select  $A = 49$  recoils with  $Q = 19$ , cutting out  $A = 48$  and 50 recoils in the same charge state.

Of critical importance was the production of a clean E/DE spectrum in the ionization chamber with little scattered beam and clean separation in  $Z$  of different isobars. The effect of the degrader foil needed to be investigated. Two different degrader foils were used in the test - a  $3.1 \text{ mg cm}^2$  Au foil and a  $1.71 \text{ mg cm}^2$  Ti foil. In both of these cases, the resulting E/DE spectrum showed very clear separation of isobars of different  $Z$ , although the use of the Au foil resulted in more scattered beam than recoils - in a ratio of about 5:1. The use of the Ti foil improved this dramatically, with a beam recoil ratio of about 1:1 in the E/DE spectrum. The results shown in Fig. I-25 correspond only to data taken with the Ti foil degrader. The ionization chamber spectrum is shown

in Fig. I-25(a). The spectrum shows a very clear separation in  $Z$ , with the recoils dominated by the expected  $A = 49$  isobars of V, Cr and Mn. In addition, the spectrum shows contamination due to charge-state ambiguities (mainly  $^{46}\text{Ti}$ ), scattered beam and higher- $Z$  recoils generated by reactions in the Ti foil. In order to clean this spectrum, an analysis using calibrated total energy ( $E$ ) and time-of-flight ( $T$ ) was undertaken.  $ET^2$  is proportional to mass, and a 2D plot of  $ET^2$  vs.  $A/Q$  can be used to separate recoils of the desired mass from charge-state ambiguities and scattered beam. The  $ET^2$  value for  $A = 49$  was determined, and a 2D gate placed on the  $ET^2$  vs.  $A/Q$  plot. The resulting ionization chamber spectrum is shown in Fig. 1(b). The result of the  $ET^2$  gating is that most of the scattered beam and charge-state ambiguities, and essentially all of the reactions from the Ti foil, have been removed.

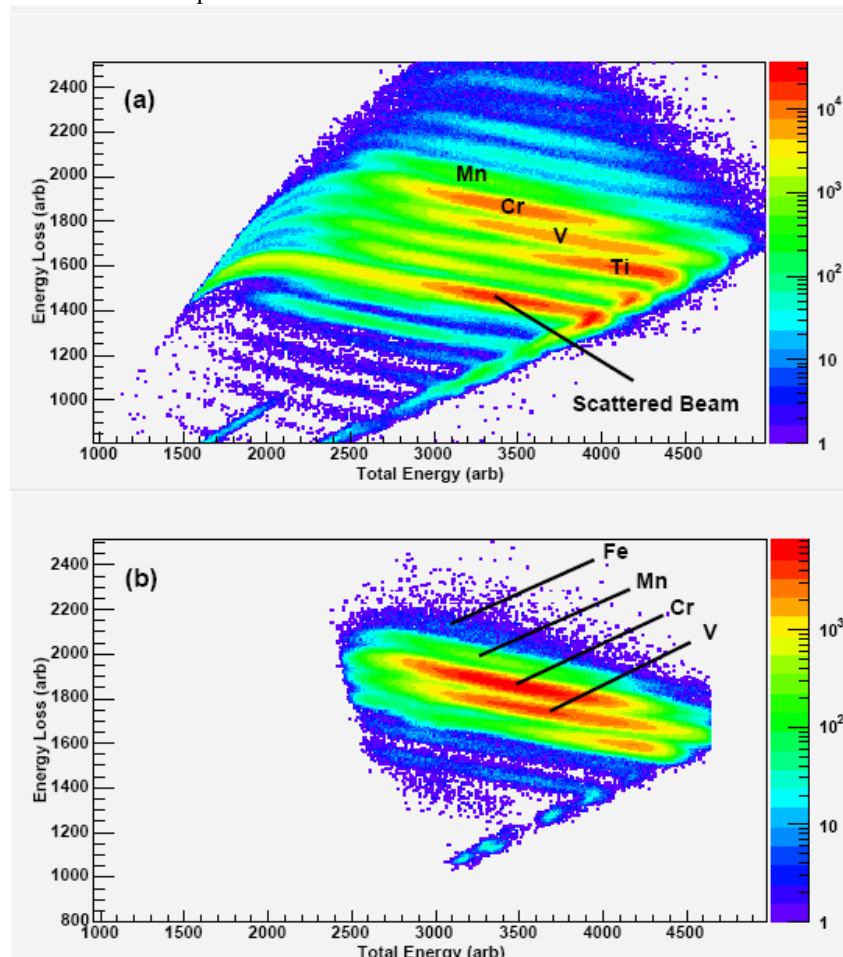


Fig. I-25. E/DE maps from the ionization spectrum, taken from data using the Ti degrader foils. (a) The raw E/DE spectrum, and (b) the E/DE spectrum gated by the  $ET^2$  value corresponding to  $A = 49$ .

The  $A = 49$  isobars now dominate the spectrum, as expected, and a clear region of counts in the expected

position for Fe recoils is now apparent. Thus, we believe that this region corresponds to mostly  $^{49}\text{Fe}$  recoils. The

number of counts in this region was determined to be around 3000 in 10 hours of beam time. Using the 250  $\mu\text{b}$  cross-section for  $^{49}\text{Fe}$  used in the original proposal, one would expect around 1500 recoils in this time assuming a 10% FMA efficiency. This seems consistent, as one would expect some fraction of the counts in the region of interest to originate from breakthrough from  $^{49}\text{Mn}$  and other residual background. Thus we are confident that the cross-section estimate is reasonable.

Gamma-spectra from the clover detector, gated by the different regions of Fig. I-25(b), are shown in Fig. I-26. This combination of 2D gates on E/DE and  $\text{ET}^2$  vs.  $A/Q$  results in extremely clean spectra of the isobars  $^{49}\text{V}$ ,  $^{49}\text{Cr}$  and  $^{49}\text{Mn}$ . All the labeled gamma rays originate from these three isobars, and the

spectra are free from contaminants other than a 511 keV peak. As would be expected, the Fe-gated spectrum has very low statistics, but is also clearly free from contamination. The comparison of the spectra of the mirror pair  $^{49}\text{Cr}/^{49}\text{Mn}$  is important, as eventually the  $^{49}\text{Fe}$  level scheme will be determined by comparison of the spectrum with that of its mirror-partner,  $^{49}\text{V}$ . Comparison of Figs. I-26(b) and (c) shows that  $^{49}\text{Mn}$  can be *just* be identified up to  $J^\pi = 23/2$  from this clean spectrum. To be confident of establishing the level scheme of  $^{49}\text{Fe}$  up to the same spin, we estimate that we need a factor of 2-3 improvement in the statistics in Fig. I-26(b) in an equivalent spectrum generated for  $^{49}\text{Fe}$ . We therefore require a factor of around 300 improvement in statistics for a good measurement. This is achievable in a full seven day Gammasphere-FMA experiment.

---

\*Keele University, Staffordshire, United Kingdom, †CLRC Daresbury Laboratory, Warrington, United Kingdom, ‡Lund University, Sweden, §University of Brighton, United Kingdom, ¶University of Surrey, United Kingdom.

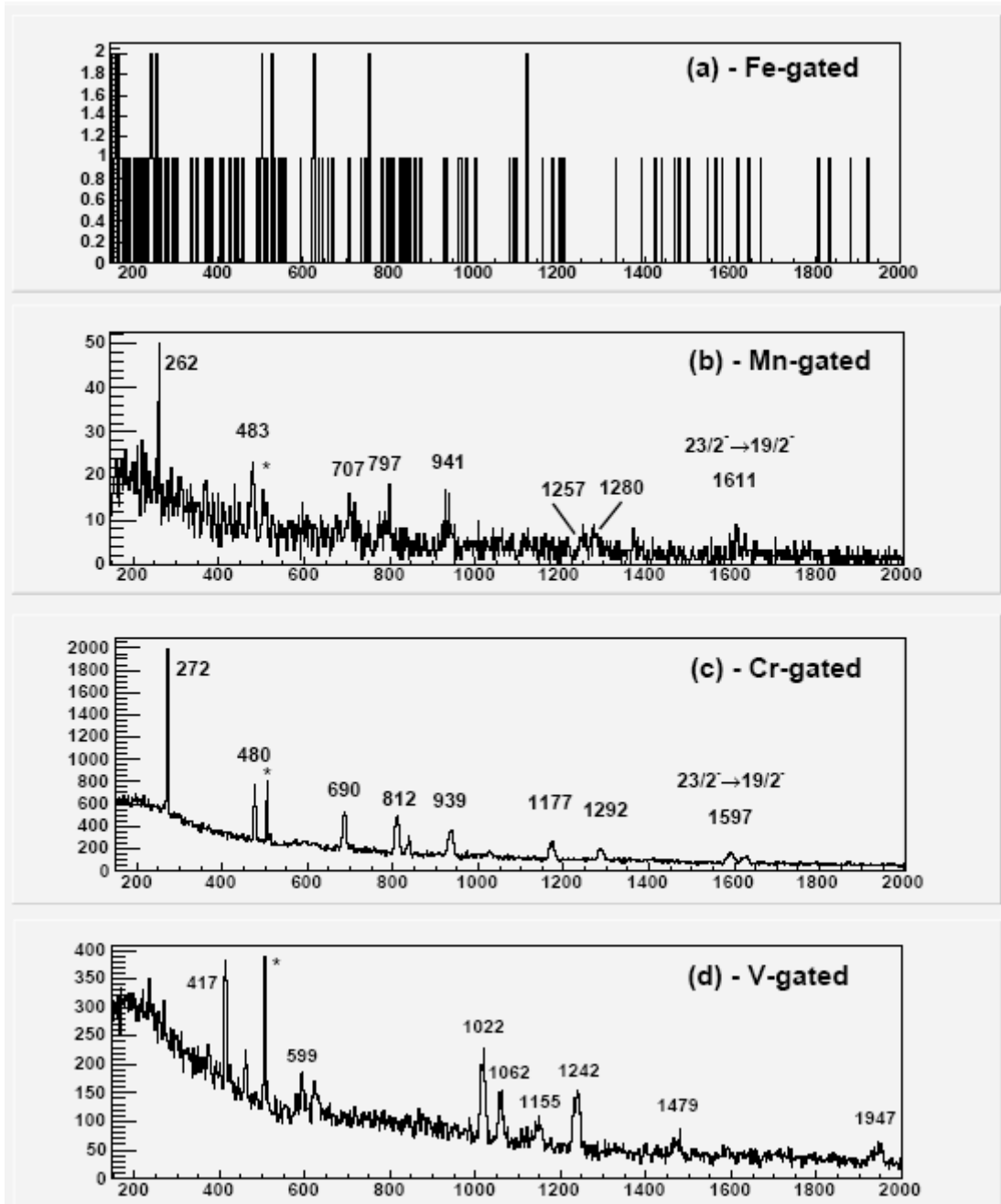


Fig. I-26. Gamma-ray spectra from the single clover detector located at 90 degrees to the beam direction. All the spectra were gated by a 2D region of the  $ET^2$  vs.  $A/Q$  plot corresponding to  $A = 49$  recoils. The individual spectra are also gated by regions of the  $E/DE$  map corresponding to (a) Fe, (b) Mn, (c) Cr and (d) V. The marked transitions are known gamma rays in the relevant  $A = 49$  isobars - (b)  $^{49}\text{Mn}$ , (c)  $^{49}\text{Cr}$  and (d)  $^{49}\text{V}$ . The \* symbol indicates the 511 keV transition.

#### d.2.4. Shape Co-Existence in $^{71}\text{Br}$ and the Question of the Groundstate Spin of $^{71}\text{Kr}$ (S. M. Fischer, C. J. Lister, D. P. Balamuth,\* P. A. Hausladen,\* T. Anderson,† D. Svelnys,† G. Mesoloras,† and D. G. Sarantites‡)

When the  $N = Z$  line approaches the proton dripline above  $^{56}\text{Ni}$  an increasing distortion of mirror symmetry is expected as the proton rich partner becomes marginally bound. Urkedal and Hamamoto<sup>1</sup> have considered  $^{71}\text{Kr}$  and suggest the distortion could lead to a different groundstate spin to its mirror partner  $^{71}\text{Br}$ , based on the reinterpretation of a  $\beta$ -decay measurement. This would be a unique situation in  $T = 1/2$  nuclei. We have performed a new "inbeam" spectroscopic measurement of  $^{71}\text{Br}$ , following the  $^{40}\text{Ca}(^{40}\text{Ca}, 2\alpha p)$  reaction at 160 MeV and using Gammasphere. Many new states have been found, with candidates for eight Nilsson bandheads below 1 MeV. Cross-linking decays tightly constrain most of the angular momentum assignments. The  $^{71}\text{Kr}$   $\beta$ -decay data, seen in the light of this new information on  $^{71}\text{Br}$ , support the original

groundstate assignment of  $^{71}\text{Kr}$  as  $J^\pi = 5/2^-$ , and as would be normally expected for the mirror partner of  $J^\pi = 5/2^-$   $^{71}\text{Br}$ .

This research is now complete and a long paper has been published in Phys. Rev. C.<sup>2</sup> The investigation revealed the importance of comparing  $^{71}\text{Br}$  to its mirror,  $^{71}\text{Kr}$ . This  $A = 71$  mirror pair is rather special, as an isomer allows ultra-sensitive clean, Doppler free spectroscopy between beam bursts. The  $^{71}\text{Br}$  isomer decay is shown in Fig. I-27. Predictions for the analogous isomer in  $^{71}\text{Kr}$  show sensitivity to the charge-symmetry-breaking "Electromagnetic-Spin-Orbit" effect,  $V_{\text{eso}}$ . Estimates indicate the isomer is lowered in  $^{71}\text{Kr}$  by  $\sim 250$  keV, close to 500 keV and with a half-life of several hundred ns. A proposal for an optimized experiment has been accepted by the ATLAS PAC.

\*Pennsylvania State University, †DePaul University, ‡Washington University.

<sup>1</sup>P. Urkedal and I. Hamamoto, Phys. Rev. C **58**, R1889 (1998).

<sup>2</sup>S. M. Fischer *et al.*, Phys. Rev. C **72**, 024321/1-16 (2005).

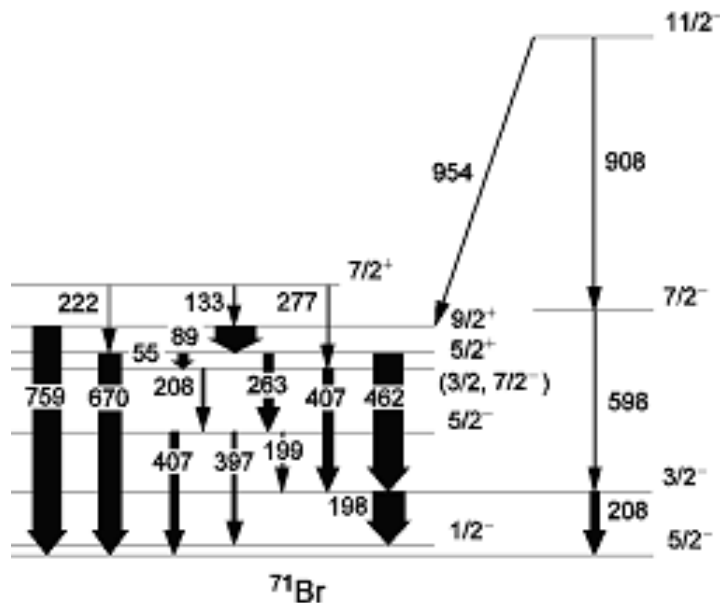


Fig I-27. The low lying levels in  $^{71}\text{Br}$ . The  $T_{1/2} = 33$  ns isomer allows ultra sensitive Doppler-free spectroscopy. In this case, three doublets of transitions were discovered, leading to a considerably modified sequence of levels. This is a perfect laboratory for testing for violation of Mirror Symmetries.

**d.2.5. Fast Alpha Decays Above  $^{100}\text{Sn}$**  (A. A. Hecht,\* C. J. Lister, C. N. Davids, D. Seweryniak, S. Zhu, N. Hoteling,† J. Palombo,† J. Shergur,† W. B. Walters,† P. J. Woods,‡ A. Heinz,§ and C. Mazzocchi¶)

Since the initial discovery of groundstate alpha decays immediately above  $^{100}\text{Sn}$ ,<sup>1</sup> in tellurium isotopes, the possibility of enhanced “superallowed” alpha decays has been often discussed. Briefly, the concept is that near the  $N = Z$  line the valence particles all occupy the same orbits, so alpha pre-formation should be enhanced relative to the classic cases of spherical alpha decay beyond  $^{208}\text{Pb}$ , for example in  $^{212}\text{Po}$ . Consequently, the reduced alpha-decay widths might be very large. Despite these possible large alpha-widths, the decay Q-values are quite modest and the absolute alpha decay rates are not high, so strong competition from  $\beta$ -decay usually occurs which makes experimental measurements difficult. Further, the nuclei lie far from stability, and the most interesting cases, those with  $N \sim Z$  lie at or even beyond the proton dripline, so can only be produced with low cross-section reactions. A number of alpha emitters beyond  $^{100}\text{Sn}$  have now been found, most recently the decay of  $^{114}\text{Ba}$ .<sup>2,3</sup> The experiments at GSI used an ISOL technique to separate ions and measure the decay modes. This technique is very sensitive, especially when molecular species are extracted from the ion source, but has limitations in extracting very short-lived ions. We have attempted to push close to the  $N = Z$  line by using the Argonne Fragment Mass Analyzer (FMA) to separate ions in-flight and enhance sensitivity for decays in the  $\mu\text{s}$  and  $\text{ms}$  half-life ranges.

Two experiments were attempted. First, the  $^{58}\text{Ni}(^{58}\text{Ni},3n)^{113}\text{Ba}$  reaction was studied at 250 and 260 MeV. This channel was estimated to have a cross-section  $\sim 5$  nb. Ions were mass separated by the FMA and implanted into a  $80 \times 80$  strip silicon DSSD. The advantage of this study is the parent is expected to be relatively long ( $\sim 100$  ms),<sup>4,6</sup> but is followed by fast subsequent alpha decays of the daughter ( $^{109}\text{Xe}$ ),<sup>7</sup> so implant-decay-decay correlations could be used. The disadvantage of this study is the long lifetime implies severe competition from  $\beta$ -decay that steals flux from the interesting

alpha-decay channels. The second experiment was to form  $^{109}\text{Xe}$  directly, using the  $^{54}\text{Fe}(^{58}\text{Ni},3n)$  reaction at 240 MeV. Here, the expected decay energy is higher, so the half-life is expected to be shorter ( $\sim 10$  ms), reducing competition from  $\beta$ -decay. However, the daughter decay, that of  $^{105}\text{Te}$ , is expected to be very fast,  $\sim 1$   $\mu\text{s}$ , so may pile-up with the decay of the parent, and suppress implant-decay-decay correlations. This strongly reduces the sensitivity of the experiment.

The experiments ran smoothly and large data sets were collected for both experiments. The former experiment ran for 89 hours with an average beam current of 9 pna. The latter study ran for 24 hours with an average current of 6 pna. Targets were  $\sim 0.5$   $\text{mg}/\text{cm}^2$  and the FMA transport efficiency for a single charge state was estimated as 8%. Both reactions produced known alpha emitters in other reaction channels which could be used to verify the correct functioning of the experiment. Data analysis is still in progress. However, no clear candidates for either of the  $N = Z + 1$  emitters  $^{113}\text{Ba}$  nor  $^{109}\text{Xe}$  could be identified, despite the fact that our estimates indicated 10-100s of decays should have been observed. It is possible that at the beam energies these experiments were run at the “3n” evaporation channel was much weaker than predicted by evaporation calculations re-scaled to experimental data. However, it would have to be  $< 1$  nb to provide a satisfactory explanation. Reaching far from stability by multi-neutron evaporation is essential for dripline spectroscopy, especially for studying nuclei immediately around  $^{100}\text{Sn}$ , so this reaction mechanism issue needs further investigation. In the case of  $^{113}\text{Ba}$ , strong competition from  $\beta$ -decay may have suppressed our observation of decay correlations. In the case of  $^{109}\text{Xe}$  decays, searches for implant-decay and implant-summing events were made, but the lack of granddaughter correlations greatly reduced our sensitivity.

This research is continuing with a goal to establishing firm limits on production cross-sections and on possible decay modes.

\*Argonne National Laboratory and University of Maryland, †University of Maryland, ‡University of Edinburgh, United Kingdom, §Yale University, ¶Oak Ridge National Laboratory.

<sup>1</sup>R. D. McFarlane and A. Siivols, Phys. Rev. Lett. **14**, 14 (1965).

<sup>2</sup>A. Guglielmetti *et al.*, Phys. Rev. C **56**, R2912 (1997).

<sup>3</sup>C. Mazzocchi *et al.*, Phys. Lett. **B352**, 29 (2002).

<sup>4</sup>S. Liran and N. Zeldes, At. Data and Nucl. Data Tables **17**, 431 (1976).

<sup>5</sup>P. Moller, J. R. Nix, and K.-L. Kratz, *ibid* **66**, 131 (1997).

<sup>6</sup>J. O. Rasmussen, *Phys. Rev.* **113**, 1593 (1959).

<sup>7</sup>G. Audi *et al.*, *Nucl. Phys.* **A729**, 337 (2003).

**d.2.6. Discovery of the Deformed Proton Emitter  $^{121}\text{Pr}$**  (C. N. Davids, D. Seweryniak, M. P. Carpenter, R. V. F. Janssens, D. Peterson, S. Sinha, S. Zhu, A. P. Robinson,\* P. J. Woods,\* A. A. Hecht,† J. Shergur,† and W. B. Walters†)

Ground state proton radioactivity has been identified in  $^{121}\text{Pr}$ . 240 MeV  $^{36}\text{Ar}$  beams were used to bombard a 0.7 mg/cm<sup>2</sup> thick  $^{92}\text{Mo}$  target, and produced  $^{121}\text{Pr}$  via the  $1p6n$  fusion-evaporation channel. The recoiling nuclei were separated from the primary beam and other contaminants by the FMA, and implanted into a double-sided silicon strip detector (DSSD). Figure I-28 shows the energy spectrum for decay events in the DSSD occurring within 30 ms of an  $A = 121$  recoil being implanted into the same quasi-pixel. The protons have an energy of

882(5) keV, and decay with a half-life of  $10^{+6}_{-3}$  ms. The estimated production cross-section is  $\sim 300$  pb. Calculations indicate that the observed decay rate is consistent with the proton occupying either the  $K = 3/2^+[422]$  or  $K = 3/2^-[541]$  deformed Nilsson orbital. Other nearby orbitals with  $K = 1/2^+[420]$  or  $K = 9/2^+[404]$  give calculated decay half-lives more than an order of magnitude too short or too long, respectively.

This work has been published as a Physical Review Letter.<sup>1</sup>

\*University of Edinburgh, United Kingdom, †University of Maryland.

<sup>1</sup>A. P. Robinson, P. J. Woods, D. Seweryniak, C. N. Davids, M. P. Carpenter, A. A. Hecht, D. Peterson, S. Sinha, W. B. Walters, and S. Zhu, *Phys. Rev. Lett.* **95**, 032502/1-4 (2005).

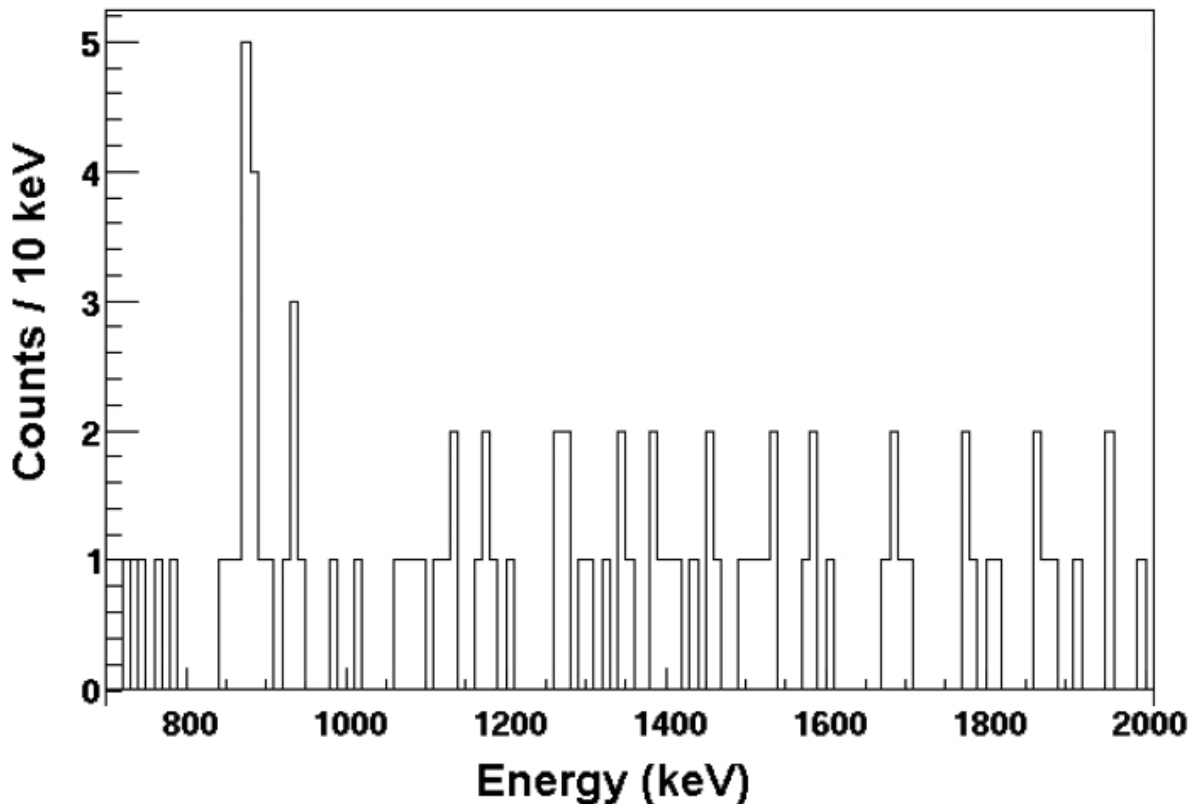


Fig. I-28. Decays in the DSSD produced using a 240 MeV  $^{36}\text{Ar}$  beam to bombard a  $^{92}\text{Mo}$  target, within 30 ms of implantation into a DSSD quasi-pixel. The ground-state proton decay peak of  $^{121}\text{Pr}$  falls at an energy of 882(5) keV.

**d.2.7. Recoil-Decay Tagging Study of  $^{146}\text{Tm}$**  (C. N. Davids, D. Seweryniak, B. Blank, M. P. Carpenter, N. Hammond, R. V. F. Janssens, G. Mukherjee, S. Sinha, A. Robinson,\* P. J. Woods,\* T. Davinson,\* Z. Liu,\* S. J. Freeman,† N. Hoteling,‡ J. Shergur,‡ W. B. Walters,‡ A. Woehr,‡ C. Scholey,§ and A. A. Sonzogni¶)

$^{146}\text{Tm}$  is an odd-odd proton emitter which lies in the transitional region between predicted deformed and near-spherical shapes. It is potentially a rich source of information regarding the role of the odd neutron in proton decay. The improved statistics in this experiment allow some of the long-standing difficulties with the level scheme of  $^{146}\text{Tm}$  to be addressed. A tentative decay scheme is shown in Fig. I-29. The most intense  $\sim 200$  ms 1122 keV transition is assigned as an  $l = 5$  transition from a  $(10^+, 9^+, 8^+)$  state based on the  $\pi h_{11/2} \nu s_{1/2}$  configuration, which agrees with previous work. As in previous work the 1192 keV transition is assigned as an  $l = 5$  transition from a  $(6^-, 5^-)$  state based on the  $\pi h_{11/2} \nu s_{1/2}$  configuration to the ground state of  $^{145}\text{Er}$ . From the present half-life measurements it appears that the 937 keV, 1010 keV and 1192 keV transitions occur from the same state, with a half-life of  $\sim 80$  ms. The neighboring  $N = 77$  isotones have a number of low lying  $3/2^+$  and  $5/2^+$  states below the  $11/2^-$  state. On the basis of this, and the delayed  $\gamma$ -rays seen in coincidence with the 937 keV and 1010 keV transitions (see Fig. I-30) the 937 keV and 1010 keV transitions are assigned as decays from the  $(6^-, 5^-)$  state in  $^{146}\text{Tm}$  to low lying  $(5/2^+)$  and  $3/2^+$  states in

$^{145}\text{Er}$ . This is the first example of decay to 3 states in the daughter nucleus from a proton emitter. The placement of the 892 keV transition is more problematic. It has previously been assigned as a decay from the  $(10^+)$  isomeric state in  $^{146}\text{Tm}$  to a  $9/2^-$  state in  $^{145}\text{Er}$ , however this assignment would require a significant admixture of the  $\pi f_{7/2}$  orbital to the emitter wave function. An alternative assignment could be the  $l = 0$  decay of a low lying  $(1^+)$  state in  $^{146}\text{Tm}$  to the ground state of  $^{145}\text{Er}$ . A similar state is seen in neighboring odd-odd isotopes.

The recoil-decay tagged prompt  $\gamma$ -ray spectra (not shown) correlated with the 892 keV and 1122 keV transitions also provide information on the origin of the 892 keV particle group. Despite the low statistics in the 892 keV spectrum, it does not contain the most intense transition correlated with the 1122 keV spectrum. This suggests that the decays occur from two separate states in  $^{146}\text{Tm}$ , rather than from the same state as in earlier work. The absence of delayed  $\gamma$ -rays in coincidence with the 892 keV transition suggests that the decay is to the ground state. A comparison of experimental partial proton decay half-lives with detailed theoretical calculations is needed to fully determine the structure of  $^{146}\text{Tm}$ .

\*University of Edinburgh, United Kingdom, †University of Manchester, United Kingdom, ‡University of Maryland, §University of Jyväskylä, Finland, ¶Brookhaven National Laboratory.

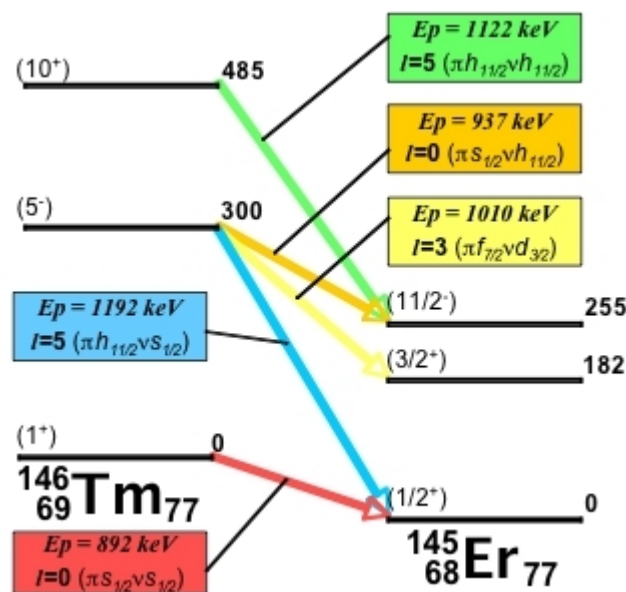


Fig. I-29. Tentative proton decay scheme for  $^{146}\text{Tm}$ .

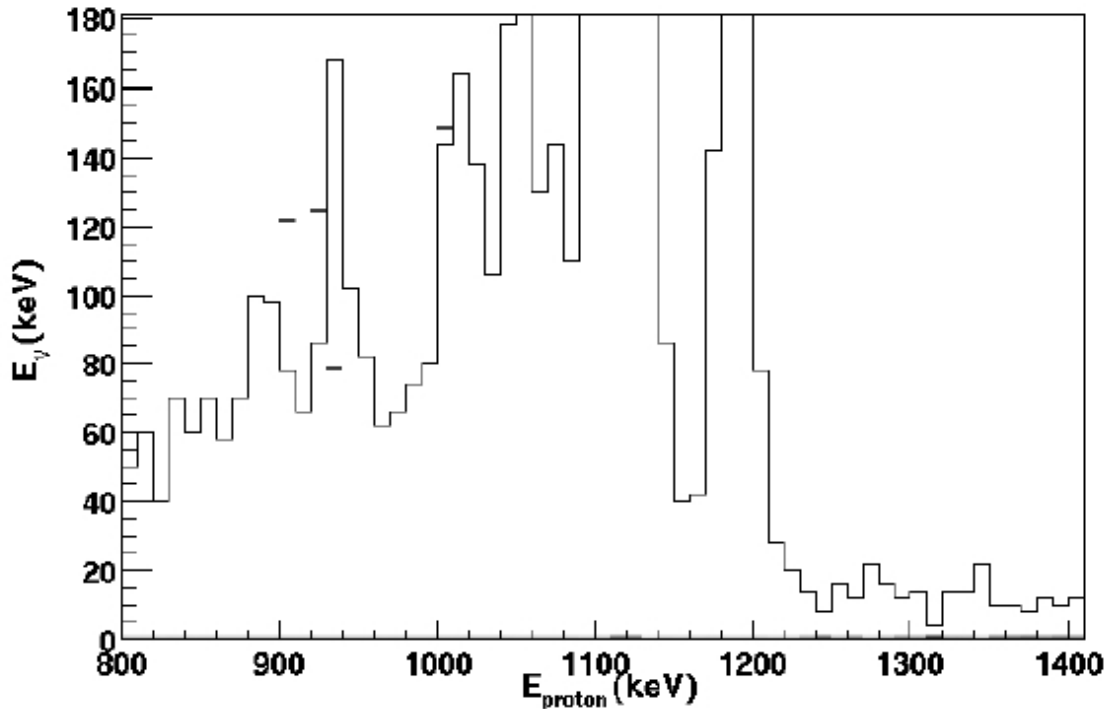


Fig. I-30. Delayed  $\gamma$ -rays in coincidence with particle decays detected at the FMA focal plane. The (4) events detected are shown as horizontal lines. The particle decay spectrum is shown overlaid.

#### d.2.8. Multi-Particle Configurations in $N = 84$ Isotones Located at the Proton Drip-

Line (D. Seweryniak, J. Uusitalo, M. P. Carpenter, C. N. Davids, R. V. F. Janssens, T. Lauritsen, C. J. Lister, D. Nisius, P. Reiter, P. Bhattacharyya,\* J. A. Cizewski,† K. Y. Ding,‡ N. Fotiades,§ A. O. Macchiavelli,¶ W. B. Walters,|| and P. J. Woods\*\*)

Excited states in the proton rich  $N = 84$  isotones  $^{156}\text{Hf}$ ,  $^{157}\text{Ta}$ , and  $^{158}\text{W}$ , were observed using  $^{102}\text{Pd}(^{58}\text{Ni}, xp2n)$  reactions at 270 MeV. Gamma rays were detected with the Gammasphere array of Compton suppressed Ge detectors coupled with the Argonne fragment mass analyzer, and were assigned to individual reaction channels using the recoil-decay tagging method. Prompt  $\gamma$ -ray cascades were

associated with the  $\alpha$  decay of both the ground state and the  $8^+$  isomeric state in  $^{156}\text{Hf}$ , the  $h_{11/2}$  state in  $^{157}\text{Ta}$ , and the  $8^+$  isomeric state in  $^{158}\text{W}$ . The level schemes were constructed for  $^{156}\text{Hf}$ ,  $^{157}\text{Ta}$ , and  $^{158}\text{W}$ . The details of the data analysis and the comparison between the proposed level schemes with the lighter  $N = 84$  isotones and the shell model calculations were published in Ref. 1.

\*Purdue University, †Argonne National Laboratory and Rutgers University, ‡Rutgers University (present address: Telecordia Technology, Piscataway, NJ 08854), §Rutgers University (present address: Los Alamos National Laboratory), ¶Lawrence Berkeley National Laboratory, ||University of Maryland, \*\*University of Edinburgh, United Kingdom

<sup>1</sup>D. Seweryniak, J. Uusitalo *et al.*, Phys. Rev. C **71**, 054319 (2005).



**d.2.9. Alpha Decay of  $^{181}\text{Pb}$**  (M. P. Carpenter, F. G. Kondev, R. V. F. Janssens, I. Ahmad, C. N. Davids, N. J. Hammond, T. L. Khoo, T. Lauritsen, C. J. Lister, G. Mukherjee, D. Seweryniak, S. Sinha, D. G. Jenkins,\* P. Raddon,\* R. Wadsworth,\* S. J. Freeman,† S. M. Fischer,‡ G. Jones,§ A. J. Larabee,¶ and A. Liechty¶)

With the return of Gammasphere to ATLAS, we have continued our program to look at proton-rich nuclei in the vicinity of the  $Z = 82$  closed proton shell. One of recent measurements utilized the  $^{90}\text{Zr} + ^{92}\text{Mo}$  reaction to produce  $^{181}\text{Tl}$  and  $^{181}\text{Pb}$  via the  $1p$  and  $1n$  channel, respectively. For this measurement, Gammasphere was coupled with the FMA to characterize both the ground and excited states in these two nuclei. At the focal plane of the FMA, the PGAC measured the mass, the DSSD detected the energies of both implants and the  $\alpha$  particles emitted from the decay of the implanted ions and associated daughter nuclides. In addition four Ge detectors surrounded the DSSD in order to measure  $\gamma$  rays in coincidence with detected particles.

$^{181}\text{Pb}$  with  $N = 99$  is the lightest odd-A Pb isotope identified thus far. In our measurement, we observe two  $\alpha$  lines at 7015(10) and 7075(10) keV with nearly equal intensity. Both of these decays are correlated with the 6580-keV  $\alpha$  decay of  $^{177}\text{Hg}$ . Our observations are in contrast to a previous result which reported observing only one  $\alpha$  line at 7065 keV.<sup>1</sup> In addition, the 7015 keV  $\alpha$  line is in coincidence with a 77 keV  $\gamma$  ray. This  $\gamma$  ray has been identified previously, resulting from the decay of an excited  $9/2^-$  state to the  $7/2^-$  ground state in  $^{177}\text{Hg}$ .<sup>2</sup> Both  $\alpha$  lines have the same half-life,  $39.6 \pm 0.9$  msec, suggesting that both are associated with the decay of the  $^{181}\text{Pb}$  ground state. While it is clear that the 7015 keV  $\alpha$  feeds the  $9/2^-$  state in  $^{177}\text{Hg}$ , an  $\alpha$ -decay feeding

directly the ground state in  $^{177}\text{Hg}$  would have an energy of  $\sim 7088$  keV. In addition, a 78-keV M1 transition is highly converted with a conversion coefficient of around four. Since the K threshold for  $Z = 80$  is at 90 keV, the majority of the emitted electrons emanate from the L-shell resulting in electron energies of  $\sim 60$  keV which is the energy difference between the two observed  $\alpha$  lines. Factoring all of this information together, it appears that the 7075 keV  $\alpha$  results from the sum of the 7015 keV  $\alpha$  and the electron emitted during the conversion process. In conclusion, we observe only one  $\alpha$  decay coming from the ground state in  $^{181}\text{Pb}$  and feeding the lowest  $9/2^-$  state in  $^{177}\text{Hg}$ . As a result, the ground state of  $^{181}\text{Pb}$  must be  $9/2^-$  as well. This is in contrast to the heavier odd-A Pb isotopes, where two  $\alpha$ -decaying states have been identified and associated with a high-spin ( $13/2^+$ ) isomer state and a low-spin ( $3/2^-$ ) ground state.

This change in the ground state results from the fact that the  $p_{1/2}$ ,  $p_{3/2}$ ,  $f_{5/2}$  and  $i_{13/2}$  orbitals should be emptied at  $N = 100$ . Below  $N = 100$ , one begins to empty either the  $h_{9/2}$  or  $f_{7/2}$  shell. Our measurements show that at  $N = 99$ , the  $h_{9/2}$  orbital lies above the  $f_{7/2}$ , which has been experimentally determined for the first time. This can be contrasted to  $^{207}\text{Pb}$  where the ordering in energy is reversed. In addition, this result shows that the  $7/2^-$  ground states in  $^{177}\text{Hg}^2$  ( $N = 97$ ) and  $^{179}\text{Hg}^3$  ( $N = 99$ ) are built on weakly deformed prolate shapes as opposed to spherical states where the expected spin/parity would be  $9/2^-$  as in  $^{181}\text{Pb}$ .

\*University of York, United Kingdom, †University of Manchester, United Kingdom, ‡DePaul University,

§University of Liverpool, United Kingdom, ¶Greenville College.

<sup>1</sup>K. S. Toth *et al.*, Phys. Rev. C **53**, 2513 (1996).

<sup>2</sup>A. Melerangi *et al.*, Phys. Rev. C **68**, 041301(R) (2003).

<sup>3</sup>F. G. Kondev *et al.*, Phys. Lett. **B528**, 221 (2002).

**d.2.10. Level Structure of  $^{181}\text{Tl}$**  (M. P. Carpenter, F. G. Kondev, R. V. F. Janssens, I. Ahmad, C. N. Davids, N. J. Hammond, T. L. Khoo, T. Lauritsen, C. J. Lister, G. Mukherjee, D. Seweryniak, S. Sinha, D. G. Jenkins,\* P. Raddon,\* R. Wadsworth,\* S. J. Freeman,† S. M. Fischer,‡ G. Jones,§ A. J. Larabee,¶ and A. Liechty¶)

With the return of Gammasphere to ATLAS, we have continued our program to look at proton rich nuclei in the vicinity of the  $Z = 82$  closed proton shell. One of

our most recent experiments utilized the  $^{90}\text{Zr} + ^{92}\text{Mo}$  reaction to produce  $^{181}\text{Tl}$  and  $^{181}\text{Pb}$  via the  $1p$  and  $1n$  channel, respectively. For this measurement,

Gammasphere was coupled with the FMA to characterize both the ground and excited states in these two nuclei. At the focal plane of the FMA, the PGAC measured the mass, the DSSD detected the energies of both the implants and the  $\alpha$  particles emitted during the decay of the implanted ions. In addition, four Ge detectors surrounded the DSSD in order to measure  $\gamma$  rays in coincidence with detected particles.

The mid-shell Tl isotopes mimic the mid-shell Pb isotopes in that structures built on spherical, oblate and prolate shapes have been established in  $^{183,185,187}\text{Tl}$ .<sup>1-3</sup> A comparison of the excitation energy of single-particle states associated with the different shapes shows that the excitation energy of the  $13/2^+$  prolate state continues to decrease as one approaches mid-shell ( $N = 102$ ) while the oblate structure built on the  $h_{9/2}$  orbital minimizes in excitation energy at  $N = 108$  and rises in energy with decreasing neutron number. In all of these isotopes the ground state remains spherical. It is an open question whether this same trend continues beyond mid-shell.

In the analysis of our Gammasphere experiment, we have followed the de-excitation of the  $i_{13/2}$  prolate band in  $^{181}\text{Tl}$  down to the 1 msec isomer built on the  $9/2^-$  oblate state. Based on our RDT measurements, most of the decay of this isomer precedes via  $\gamma$  emission to the ground state while a small  $\alpha$  decaying branch directly feeds an excited  $9/2^-$  state in the daughter nucleus,  $^{177}\text{Au}$ . Unfortunately, our measurement was not sensitive to the  $\gamma$  decay of the isomer to the spherical ground state. However, in a recent measurement with the FMA and two clover detectors placed at its focal plane, we were able to measure the gamma decay of this isomer and thus establish its excitation energy at 834 keV. A partial level scheme of our results is given in Fig. I-31 showing the gamma decay path starting from the  $i_{13/2}$  rotational down to the ground state. These results establish that both the oblate structure and the  $i_{13/2}$  prolate band rise in excitation energy when compared to the same states in  $^{183}\text{Tl}$ . In the case of the prolate structures, this is the same trend observed for the prolate bands in the even-even Pb and Hg isotopes.

\*University of York, United Kingdom, †University of Manchester, United Kingdom, ‡DePaul University, §University of Liverpool, United Kingdom, ¶Greenville College.

<sup>1</sup>W. Reviol *et al.*, Phys. Rev. C **61**, 044310 (2000).

<sup>2</sup>M. Muikku *et al.*, Phys. Rev. C **64**, 044308 (2002).

<sup>3</sup>G. J. Lane *et al.*, Nucl. Phys. **A586**, 316 (1995).

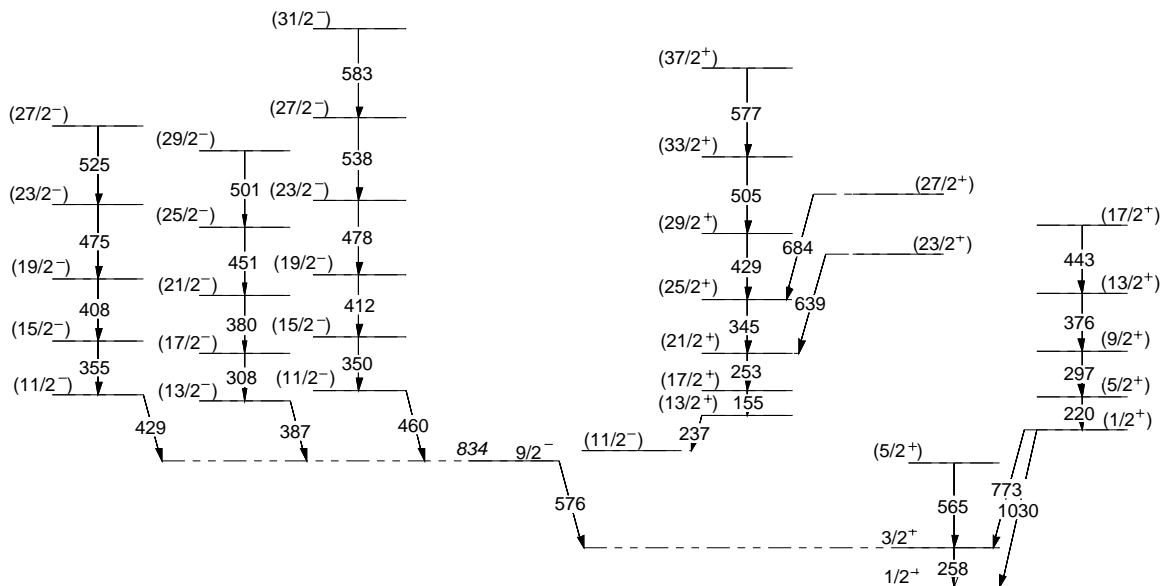


Fig. I-31. Partial level scheme for  $^{181}\text{Tl}$  deduced from this work.